

A Microfluidic Mixer for Chaotic Mixing of Magnetic Particles

M. Zolgharni, S. M. Azimi, M. R. Bahmanyar and W. Balachandran

School of Engineering and Design, Brunel University
Uxbridge, Middlesex, UB8 3PH, UK, Massoud.Zolgharni@brunel.ac.uk

ABSTRACT

A numerical simulation is carried out in order to investigate the efficiency of a microfluidic mixer for chaotic mixing of the magnetic particles. Lagrangian tracking method is utilized to obtain the trajectories of the particles in the mixer domain. Two characterizing indices are computed for a range of the operating parameters of the mixer. Intensity of segregation is calculated to measure the ability of the device to spread the particles and to obtain the local concentration. Moreover, in order to examine the chaotic features in the micro-mixer, largest Lyapunov exponent is computed as the supplemental characterizing index. Simulation results show that optimum operating conditions for the mixer is obtained when the Strouhal number is less than 0.6, which corresponds to the largest Lyapunov exponent of about 0.37.

Keywords: microfluidic, chaotic mixing, magnetic particles

1 INTRODUCTION

In biological microfluidic platforms, functionalized micron-sized magnetic particles are prevalently used for selective isolation of bio-entities from their native environment [1-2]. Prior to separation of the bio-entity/particle complex from contaminants, magnetic particles must be distributed throughout the bio-fluidic solution containing target entities. This is carried out by a mixing process which results in tagging of the target with magnetic particles.

However, in such microfluidic systems mixing is not a trivial task due to the fact that these devices usually operate under low Reynolds number flows where it is not possible to create turbulence to enhance the mixing and flow is unavoidably laminar. In such cases, diffusion at the molecular scale becomes the sole mechanism of mixing which takes considerable time and therefore, limits the performance of the mixer. Particularly in biological assay systems, diffusion of bio-entities such as cell and protein turns into a less efficient process than that of water-soluble entities. Therefore, alternative mixing mechanisms need to be realized in order to enhance the performance of the micro-scale devices. While lamination which relies on the idea of reducing the diffusion length using narrow mixing channel, is not an appropriate solution for particle laden fluids, chaotic mixing seems to be a promising method. The purpose of this study is to examine the efficiency of a chaotic micro-mixer through numerical simulations.

2 CONCEPT OF THE MIXER

The burst-view of the mixer is depicted in figure 1a. A straight channel with two embedded serpentine conductors beneath the channel is utilized to produce the chaotic pattern in the motion of particles. Two flows; target cells suspension and the particle laden buffer, are introduced into the channel and manipulated by pressure-driven flow (see figure 1b). While the cells follow the mainstream in upper half section of the channel, the motion of magnetic particles is affected by both the surrounding flow field and the localized time-dependent magnetic field generated by sequential activation of two serpentine conductors.

The mixing operation cycle consists of two phases. In the first half cycle, one of the conductor arrays is switched on while the other one is off. In the next half cycle, the status of conductor arrays is reversed as shown in figure 2. T is the length of period and T_p is the length of a half-cycle or phase. Each mixing unit consists of two adjacent teeth from opposite conductor arrays and the mixer is composed of a series of such mixing units which are connected together. By using a proper periodical current density and structural geometry, chaotic patterns can be produced in the particles' motion which leads to their spreading in the channel. A full description of the mixer concept and dimensions can be found in Zolgharni *et al* [3].

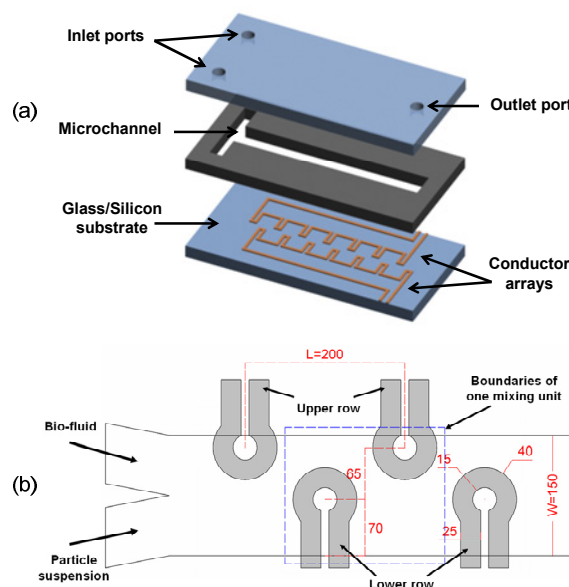


Figure 1: Concept of the mixer; (a) burst-view, (b) top view of mixer comprising one mixing unit.

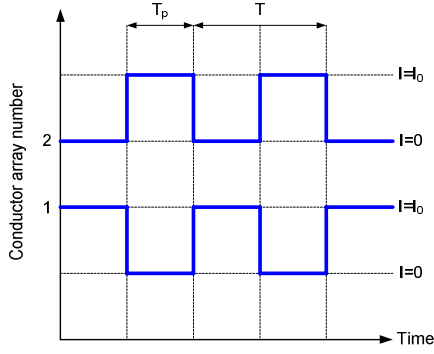


Figure 2: Control signal in the mixer.

3 NUMERICAL SIMULATIONS

3.1 Magnetic Forces

Magnetic forces are generated by the current-fed conductors embedded beneath the channel. The magnetic force on particles is a function of the external magnetic field gradient and the magnetization of the particle. Particles are assumed to be linearly magnetized with their magnetic moment magnitude increasing in the direction of the external field. In de-ionized water, the magnetic force exerted on the individual particles can be described by [4]:

$$F_m = 0.25\pi\mu_0 d^3 \frac{\mu_r - 1}{\mu_r + 2} \nabla H^2 \quad (1)$$

where F_m is magnetic force, H is the external magnetic field, d is the diameter of the particle, μ_r is relative permeability of the particle and μ_0 is permeability of the vacuum. Relative permeability and diameter of the reference particle used in this study (M-280, Dynabeads, Dynal, Oslo, Norway) are $2.83 \mu\text{m}$ and 1.76 , respectively.

Figure 3a illustrates one mixing unit with its magnetic field generated close to the circular tip of the conductor array during a half cycle of activation. The colour-map represents variations in the magnetic field intensity at a plane $10 \mu\text{m}$ above the surface of the conductor where the maximum magnitude of the field is about 6000 A/m at the centre of the circular tip (point P). Figures 3b and 3c show the magnitude of the total magnetic field ($H = (H_x^2 + H_y^2)^{1/2}$) in x-y plane along two lines A-A and B-B, respectively. Graphs show the field at different heights above the conductor and as expected, the closer to the conductor, the stronger the magnetic field can be observed.

Particles are attracted towards higher magnetic field regions. It is worth noting that the magnetic force is three-dimensional and the z component of the force is downward which pulls the particles towards the bottom of the channel and restrict their motion to a two-dimensional pattern. In fact, this component has no contribution to the chaotic

motion of the particles and is assumed not to be influential on the process of mixing. Therefore, a two-dimensional simulation is conducted where the magnetic forces close to the surface of the channel's bottom are of interest.

3.2 Advection of the Particles in the Media

Motion of the particles relative to the fluid solution can be considered as a creeping flow and therefore, drag force on the particle may be evaluated by Stokes' law. Total velocity of the particle at each moment (V_p) is the sum of velocity due to fluid field (V_f) and velocity due to the magnetic field (V_m):

$$V_p = V_f + \frac{F_m}{3\pi\mu d} \quad (2)$$

where μ is dynamic viscosity and d is the diameter of the particle.

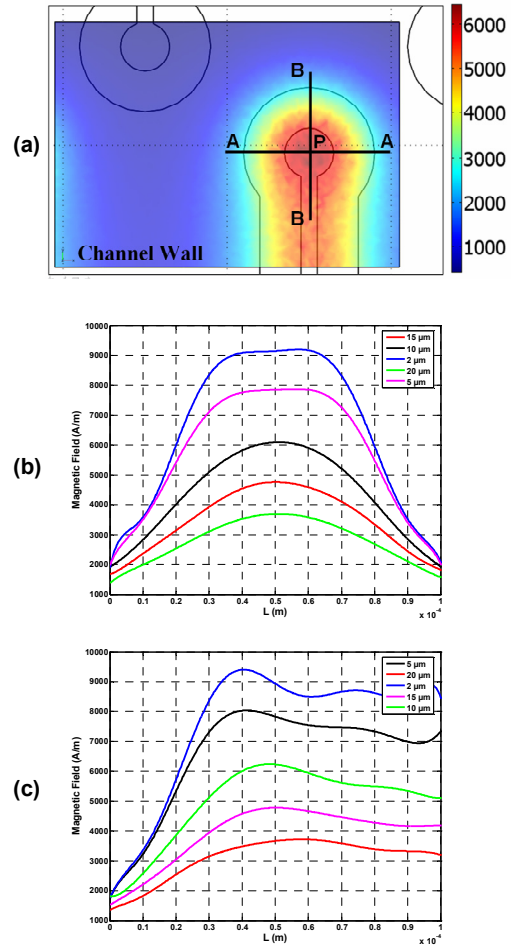


Figure 3: Magnetic field near the tip of one tooth during a single phase of activation; (a) colour-map of the field in A/m, (b) & (c) magnitude of the field at different heights above the conductor along lines A-A and B-B, respectively.

3.3 Simulation Procedure and Parameters

Numerical procedure consists of two steps: first, the steady-state velocity field of an incompressible Newtonian fluid and time-dependent magnetic field are computed and velocities of the particles due to the fluid and magnetic fields are extracted. Then Lagrangian trajectories of particles are evaluated by integrating the sum of velocities using Euler integration method. Simulation is conducted assuming that there are no magnetic or hydrodynamic interactions between particles (one-way coupling). This assumption is valid for small particles at low concentration in suspension. Trajectories of cells are obtained using the same Lagrangian tracking method as for magnetic particles, with the exception that cells are magnetically inactive and simply follow the mainstream in the fluid field. Biological cells are considered to be spheres of 1 μm diameter. In order to characterize the mixing efficiency, the effect of variation of two driving parameters; namely the bulk flow velocity and frequency of the current injection, are investigated. The ratio of these driving parameters is defined as a dimensionless number St (Strouhal number):

$$St = \frac{fL}{V} \quad (3)$$

where f is the frequency, L is the characteristic length, and V is the mean velocity of the fluid.

4 CHARACTERIZATION

A quantitative criterion to characterize the degree of mixing is the so-called “discrete intensity of segregation” which represents the ability of the system to spread the magnetic particles. Moreover, a common definition of mixing quality is based on the inspection of chaotic regimes developed in the mixer and calculating the Lyapunov exponent is a standard method of investigating chaos.

4.1 Particle Dispersion

Intensity of segregation is the variance of the concentration distribution. In fact, this index measures the deviation of local concentration from the ideal situation (i.e., homogeneous mixture) and is defined as [3]:

$$I_s = \frac{1}{\bar{C}(1-\bar{C})} \frac{1}{N} \sum_{i=1}^N (C_i - \bar{C})^2, \quad \bar{C} = \frac{1}{N} \sum_{i=1}^N C_i \quad (4)$$

where N is the number of cells, C_i is the concentration of cell i , and \bar{C} is the mean concentration over the section. For un-mixed distributions, the intensity of segregation is equal to 1. When the concentration in all cells approaches its overall average value which corresponds to optimal dispersion, I_s equals 0. However, for all other scenarios

$0 < I_s < 1$. In this study distribution of the magnetic particles is used to compute the intensity of segregation. A lump of 500 particles was injected in the lower half of the channel and I_s was computed along the channel length at various sections. At each section, a column of the cells was taken into account, thereby assessing dispersion of the particles across the channel width. I_s was computed over two mixing units for a wide range of driving parameters and the average value was obtained for each status. Comparison of these values allows revealing the driving parameters that perform more efficiently.

4.2 Lyapunov Exponent

Calculation of the Lyapunov exponent can be used to detect the incidence of chaos, measure its extent, and investigate the relationships between various affecting parameters and chaos. In this study, it is used to quantify the chaotic advection of magnetic particles. Sprott’s method is used to calculate the largest Lyapunov exponent (λ_1) which utilizes the general idea of tracking two initially close particles, and calculates average logarithmic rate of separation of the two particles. A full description of this method can found in Sprott [5]. A lump of 21 particles are uniformly distributed in upper half of the first mixing unit as the initial positions and λ_1 is calculated for each individual particle. In order to quantify the extent of chaos over the entire domain in the upper section (where cells exist), the average of λ_1 s of 21 particles is taken.

5 RESULTS AND DISCUSSION

A typical effect of the magnetic actuation is shown in figure 4. Particles and cells enter the first mixing unit from the left in upper and lower halves of the section, respectively. When there is no magnetic actuation, both cells and particles remain in their initial section and follow the streamlines of the parabolic velocity profile in Poiseuille flow as shown in figure 4a. However, when the external field is applied ($St=0.4$, $V=40 \mu\text{m/s}$), particles travel across the streamlines as well as the interface and spread in upper section of the channel (see figure 4b where continuous lines represent fluid streamlines and dimensions are normalized to the characteristic length).

Figure 5 illustrates the convergence of λ_1 versus time for one particle with two different driving parameters and also in the absence of the external field. Without magnetic perturbation, λ_1 converges to zero which indicates a steady flow. At $St=0.2$ and bulk fluid velocity of 35 $\mu\text{m/s}$ it converges to a constant value of about 0.45 whereas at velocity of 40 $\mu\text{m/s}$, this value is about 0.19. Therefore, it can be inferred that in the former operating condition, the system shows a stronger chaotic behaviour. Close observation of the graphs reveals that at the end of each phase (half cycle), quick changes occur in the value of λ_1 when the particles are re-attracted towards the next conductor tooth.

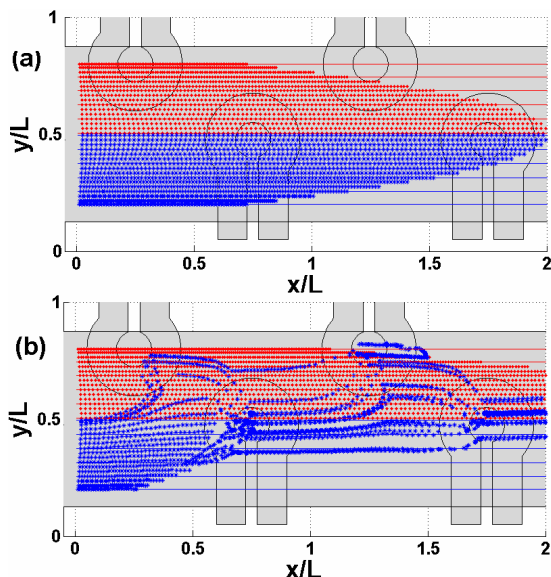


Figure 4: Advection of cells and particles within two mixing units: (a) without external perturbation, (b) with magnetic perturbation ($St=0.4, V=40 \mu\text{m/s}$). Continuous lines represent fluid streamlines and dimensions are normalized to the characteristic length.

Figure 6a and 6b show the variation of the intensity of segregation and largest Lyapunov exponent against driving parameters, respectively. The global variations of λ_1 and I_s are almost identical for different bulk flow velocities. Both characterizing indices show a good agreement; an increase in chaos leads to an increase in particle dispersion in the mixer domain. The maxima for particle dispersion happens around the Strouhal number of 0.4, while the minimum occurs at $St=0.9$. It should be noted that the values for the intensity of segregation are the mean values over the first two mixing units and do not represent the ultimate efficiency of the mixer. Maximum values for λ_1 is realized at $St=0.4$ which is 0.37.

6 CONCLUSION

A numerical simulation is performed in order to investigate the efficiency of a microfluidic mixer for chaotic mixing of the magnetic particles. Lagrangian tracking method is utilized to obtain the trajectories of the particles in the mixer domain. Intensity of the segregation is calculated to measure the ability of the device to spread the particles and largest Lyapunov exponent is computed as the supplemental characterizing index. Both characterizing indices show a good agreement; an increase in chaos leads to an increase in particle dispersion in the mixer domain. Simulation results show that optimum operating conditions for the mixer is obtained when the Strouhal number is less than 0.6, which corresponds to the largest Lyapunov exponent of about 0.37.

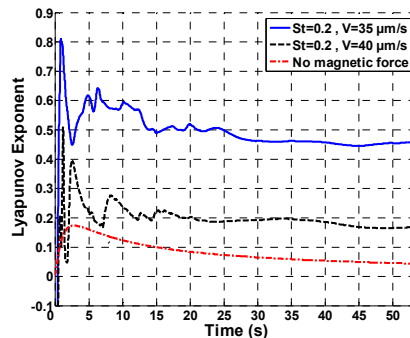


Figure 5: Convergence of the largest Lyapunov exponent for one particle.

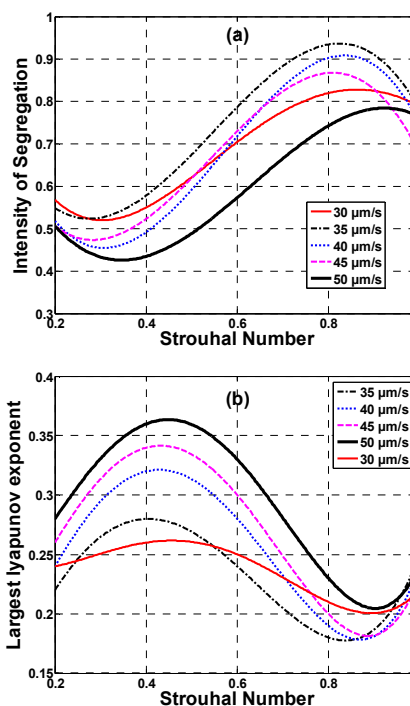


Figure 6: Variation of characterizing indices versus different system operating conditions; (a) intensity of segregation, (b) largest Lyapunov exponent.

REFERENCES

- [1] J.W. Choi, T.M. Liakopoulos and C.H. Ahn, *Biosens Bioelectron* 16(6):409–416, 2001.
- [2] Q. Ramadan, V. Samper, D. Poenar and C. Yu, *Biomed Microdevices* 8:151–158, 2006.
- [3] M. Zolgharni, S.M. Azimi, M.R. Bahmanyar and W. Balachandran, *Microfluid Nanofluid*, 2007 (in press). doi:10.1007/s10404-007-0160-9.
- [4] T.B. Jones, *Electromechanics of particles*. Cambridge University Press, Cambridge, 1995.
- [5] J.C. Sprott, *Chaos and time-series analysis*. Oxford University Press, Oxford, 2003.